Extended investigations of isotope effects on ECRH plasma in LHD

K. Tanaka[1,2], M. Nakata[1,3], Y. Ohtani[4], T. Tokuzawa[1], H. Yamada[1,3], F. Warmer[5], M. Nunami[1,3], S. Satake[1,2], T. Tala[6], T. Tsujimura[1], Y. Takemura[1,3], T. Kinoshita[2], H. Takahashi[1,3], M. Yokoyama[1,3], R. Seki[1,3], H. Igami[1], Y. Yoshimura[1], S. Kubo[1], T. Shimozuma[1], T. Akiyama[7], I. Yamada[1], R. Yasuhara[1,3], H. Funaba[1], M. Yoshinuma[1], K. Ida[1,3], M. Goto[1,3], G. Motojima[1,3], M. Shoji[1], S.Masuzaki[1], C.A. Michael[8], L.N. Vacheslavov[9,10], M. Osakabe[1,3], T. Morisaki[1,3] and LHD experiment group[1]

[1] National Institute for Fusion Science, National Institutes of Natural Sciences, Toki, Gifu, 509-5292, Japan

[2] Kyushu University, Department of Advanced Energy Engineering, Kasuga, Fukuoka, 816-8580, Japan

[3] SOKENDAI (The Graduate University for Advanced Studies), Toki, Gifu, 509-5292, Japan

[4] National Institutes for Quantum and Radiological Science and Technology, Naka, Japan

[5] Max-Planck-Institut für Plasmaphysik, Greifswald, Germany

[6] VTT, P.O. Box 1000, FI-02044 VTT, Espoo, Finland

[7] General Atomics, San Diego, California, USA

[8] University of California-Los Angeles, Los Angeles, California, USA

[9] Budker Institute of Nuclear Physics, 630090 Novosibirsk, Russian Federation

[10] Novosibirsk State University, Novosibirsk 630090, Russian Federation

E-mail: ktanaka@nifs.ac.jp

Abstract

Isotope effects of ECRH plasma in LHD were investigated in detail. A clear difference of transport and turbulence characteristics in H and D plasmas was found in the core region, with normalized radius $\rho<0.8$ in high collisionality regime. On the other hand, differences of transport and turbulence were relatively small in low collisionality regime. Power balance analysis and neoclassical calculation showed a reduction of the anomalous contribution to electron and ion transport in D plasma compared with H plasma in the high collisionality regime. In core region, density modulation experiments also showed more reduced particle diffusion in D plasma than in H plasma, in the high collisionality regime. Ion scale turbulence was clearly reduced at $\rho < 0.8$ in high collisionality

regime in D plasma compared with H plasma. The gyrokinetic linear analyses showed that the dominant instability ρ =0. 5 and 0.8 were ion temperature gradient mode (ITG). The linear growth rate of ITG was reduced in high D plasma than in H plasma. This is due to the lower normalized ion temperature gradient and density gradient. More hollowed density profile in D plasma is likely to be the key control parameter. Present analyses suggest that anomalous process play a role to make hollower density profiles in D plasma rather than neoclassical process. Electron scale turbulence were also investigated from the measurements and linear gyrokinetic simulations.

1. Introduction

Isotope effects are important issues for predicting ITER operation and for future reactor design. In LHD, deuterium experimental campaign started in 2017 and an extensive study of isotope effects is now under investigation. In this paper, experimental investigation of isotope effects on transport and turbulence in LHD ECRH plasma is reported. LHD has several advantages for the isotope effects study. Firstly, stationary discharges, which are free from MHD or macroscopic instabilities such as sawteething, are possible. Secondly, the edge pedestal is small and ELM like edge instability does not appear in most of the experimental conditions. Thirdly, there is no clear confinement transition such as L-H transition in tokamak in most of the experimental regimes. Fourthly, superconducting magnets do not require the cooling of the coils after discharge, thus, plasma discharge is possible every three minutes. Accumulation of dataset is relatively easy. Fifthly, plasma profiles including turbulence are well diagnosed by excellent diagnostics. These enable accumulation of plenty of data set in hydrogen (H) and deuterium (D) plasma under almost identical conditions. In tokamak, the H mode threshold power is lower in D plasma than in H plasma [1]. In H mode, higher edge pedestal temperature resulted in higher core temperature in D plasma than in H plasma due to the profile stiffness [2,3]. While in L mode, global energy confinement is better in D plasma, however local power balance analyses does not show clear improvements in core region in ECRH plasma [4] and NBI plasma [5]. These results in tokamak suggest that better confinement characteristics mainly originate from edge pedestal region. Thus, from the physics point of view, LHD without clear edge pedestal can be a good reference regarding the isotope effects in core region.

In LHD, there are several reports in deuterium experiments and isotope effects. A 10keV ion temperature was achieved by NBI in deuterium helium mixed plasma with carbon pellet injection [6]. The better accessibility to the ion ITB and reduced ion transport in pure D plasma than in pure H plasma were reported [7, 8]. In non-ITB normal confinement NBI plasma, dimensionally identical experiments adjusting ρ*, ν* and β were performed [9]. The results in ref.9 indicate that the normalized energy confinement time shows gyro-Bohm characteristics and co-existence of positive ion mass dependence [9]. The LHD NBI plasma showed that better confinement characteristics compared with pure gyro Bohm prediction.

In ECRH plasma of LHD, there are reports regarding experimental observation of isotope effects [6, 10, 11]. In the internal electron transport barrier plasma, lower heating power was necessary in D plasma than in H plasma [6]. The direction of tangential injection affects isotope effects of energy transport [6,10]. This can be partly due to the stochastization of closed flux surface due to ECH driven current [6, 12]. Scaling of global energy confinement times (τ_E) [10, 11], global particle confinement times (τ_P) [11] and initial results of turbulence characteristics [11] were reported. In the previous report, the reduced electron heat transport was not found from the data set of power balance analyses[11]. In this report, power balance analyses were performed for the newly obtained dataset. In addition, isotope effects of particle transports were investigated from density modulation experiments.

In this paper, investigation of transport and turbulence response in H and D plasma are reported in more detail. The turbulence is a key physics quantity to understanding the isotope effects. Also, analyses targets are focused on ECRH plasma. ECRH does not have any technical difficulty in adjusting heating condition in H and D plasma. On the other hand, from the technical point of view, NBI has technical difficulties to adjust the heating condition, because heavier ion mass results in higher heating power. From the physics point of view, differences of fast ion distribution in H and D plasma can affect the turbulence stability. Thus, ECRH plasma is suitable for the understanding the role of ion species on transport and turbulence.

In section 2, characteristics of turbulence and transports under identical heating conditions in H and D plasma are described. The gyrokinetic linear analyses are performed for discharges in H and D plasma. The results of section 2 indicate the importance of particle transport. Thus, for the understanding of isotope effects of particle transports, density modulation experiments were performed. The results are described in Section 3. Finally, the summary is shown in section 4.

2. Experimental results under identical conditions

In this section, detailed comparison of ECRH plasma in H and D plasma are shown. Purity of H and D are almost 100%. The ratio between H and D was estimated by Hα amd Dα intensity ratio by using narrow band width spectrometer distinguishing Hα and Dα. There was He contamination, which was approximately 5~10%. He contamination was estimated by spectroscopy calibrated for HeI, Hα and Dα lines. The toroidal magnetic field on axis was 2.75T. The magnetic axis position (R_{ax}) was 3.6m. This R_{ax} is the so-called inward shifted configuration. In LHD, the distance between plasma and helical winding coils are different depending on R_{ax}. Then, R_{ax} affects magnetic parameters such as toroidal magnetic ripple, helical magnetic ripple, magnetic curvature, safety factor, and magnetic shear. These magnetic properties affect transport and MHD stabilities. The R_{ax}=3.6m are characterized by the configuration with low magnetic helical ripple and strong magnetic hill. The low magnetic helical ripple results in lowering neoclassical and anomalous

transport[13] . The strong magnetic hill results in MHD unstable. However, since the volume averaged beta was low, which is less than 0.6%, the strong magnetic hill did not affect plasma performance. The plasma are stationary and free from macroscopic MHD instability. The datasets are suitable to investigate the isotope effects on transport.

The heating was 154GHz second harmonic resonant heating by using two gyrotrons. The total power was 1.97MW in H discharge and 2.05MW in D discharge. The small difference of power is due to the difference of gyrotron condition on the different experimental day. Two gyrotrons were almost the same power at 1MW. The 154GHz microwaves were injected tangentially. The injection directions are co and counter direction to Bt and EC driven currents were cancelled out. In the previous study, tangential injection affects transports and magnetic topology [6,10,12]. Thus, these effects are removed. In LHD, presently perpendicular injections are not preferred. This is because unabsorbed microwave hits cryo-sorption pump, which is located on the torus inside wall. Resonance position is at ρ (normalized position) =0.1 both in H and D plasma. More than 90% in low density (line averaged density (n_{e_bar})<1.5x10^{19}m^{-3}) and more than 80% in high density (n_{e_bar}~3x10^{19}m^{-3}) were absorbed in the first injection path. Short pulse (20ms) neutral beam was injected for the T_i and Er measurements every 400msec, but this did not affect plasma parameter. Above mentioned identical conditions were carried out for the precise comparison of transport and turbulence in H and D plasma. Keeping heating condition same, the external gas fueling was changed to scan the density so that isotope effects could be investigated in detail. The dataset in Section 2 was obtained in the 2nd deuterium campaign in 2018-2019.

2.1 General view of H and D comparison under identical condition

Figure 1 shows comparison of time trace of ECRH plasma. Two pairs of the cases, which are low density (n_{e_bar}=1.5x10^{19}m^{-3}) and high density (n_{e_bar}=3x10^{19}m^{-3}), are shown. As shown in Fig.1 (a-1) and (b-1) n_{ebar}, was adjusted to be almost identical.

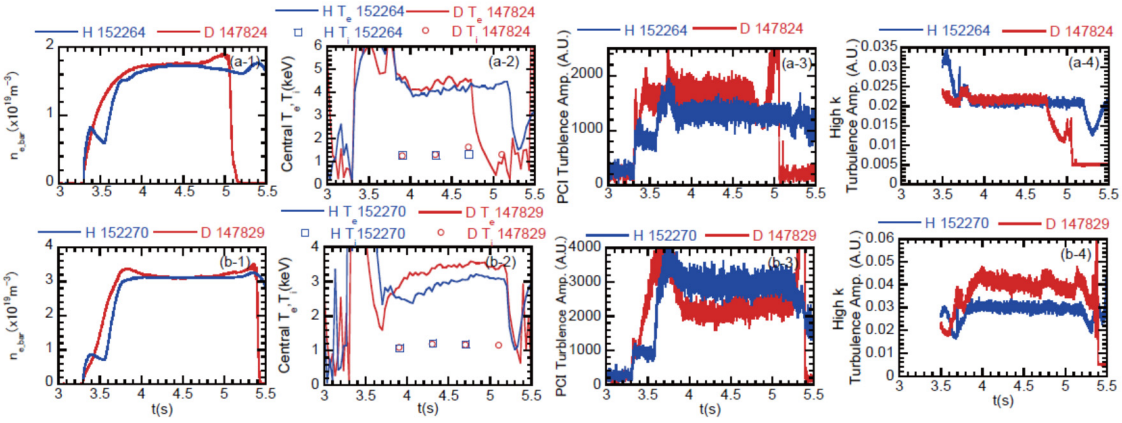

FIG.1 Comparison of time trace in (a) low and (b) high density.
(a-1),(b-1); line averaged density, (a-2),(b-2);central electron and ion temperature at ρ=0~0.2 measured by Thomson scattering and CXRS, (a-3),(b-3); line integrated fluctuation amplitude for 20-500kHz by 2D-PCI, ρ>0.4, k=0.1~0.8mm^{-1}, (a-4),(b-4); back scattering amplitude for 20-500kHz k=3~4mm^{-1}, ρ=0.7-0.8

As shown in Fig.1 (a-2), central T_e and T_i are almost identical in H and D low density shots. The deposition power was 1.91MW in H plasma, and 1.87MW in D plasma. The global energy confinement time (τ_E) was 0.192sec in H plasma and 0.203sec in D plasma. For the estimation of τ_E, diamagnetic stored energy was used. τ_E was 5% better in D plasma. The global confinement time (τ_P) was estimated by the ratio between n_{e_bar} and particle source, which is sum of Hα, Dα and HeI line. The spectrum width of spectroscopy was wider than the difference of the Hα, Dα line. Thus, both lines of were Hα, Dα measured together. The intensity between Hα, Dα mixture lines and HeI line were relatively calibrated. Thus total particle source was estimated from the sum of Hα, Dα and HeI. These measurements were performed in line integration at 10 different toroidal sections. However, volume integration quantities were difficult to estimate. Thus, only a relative estimate of τ_P was possible [11]. The estimated τ_P was 24% worse in D plasma than H plasma.

As shown in Fig.1 (b-2), in high density cases, central T_e was clearly higher in D plasma, while central T_i was almost identical. The absorption power was 1.83MW in H plasma and 1.73MW in D plasma. τ_E was 0.243sec in H plasma and 0.276sec in D plasma. τ_E was 14% better in D plasma. The improvement of τ_E was clearer in high density case. τ_P was 21% worse in D plasma than in H plasma. The degradation of τ_P in D plasma was almost the same in low and high density cases.

The scaling studies for τ_E and τ_P were carried out for the dataset in the first deuterium campaign in 2017 [11]. The results showed 16% better τ_E and 20% degraded τ_P in D plasma compared with H plasma. The results of the 2nd deuterium campaign almost reproduce previous scaling study.

Figure 1 (a-3) and (b-3) show time trace of turbulence amplitude measured by two dimensional phase contrast imaging (2D-PCI) [14, 15]. Figure 1 (a-4) and (b-4) show time trace of turbulence amplitude measured by high backward scattering (high k BS) [16].

2D-PCI measures turbulence, of which wavenumber is 0.1 ~0.8mm^{-1} and frequency is 20~500kHz. The measured k region is region of ion scale turbulence, such as ion temperature gradient mode (ITG) and trapped electron mode (TEM). The vertically injected the wavelength 10.6μm CO_2 laser beam passes at ρ = 0.35 [14]. The line integrated turbulence was measured by two dimensional detector. Then, image analysis of 2D turbulence picture can provide radial profile of turbulence. Figure 1 (a-3) and (b-3) shows line integrated turbulence amplitude, which contains turbulence at ρ > 0.35.

High k BS measures turbulence, of which wavenumber is 3~4mm^{-1} and frequency is 20~500kHz. The 90GHz (wavelength 3.3mm) microwave was injected and scattered components by k=3~4mm^{-1} were detected. The scattering angle is 170 degree, therefore, this diagnostics is called backward

scattering. It is strong contrast, in PCI, scattering angle for k=0.1-0.8mm^{-1} was less than 1 degree and scattering process was extreme forward scattering. The optical path of both injection and scattered radiations were calculated by ray tracing code. The measured k region of high k BS is approximately one order magnitude higher than turbulence measured by 2D-PCI.
The measured k region of high k BS is close to electron scale electron temperature gradient mode (ETG) region. The scattering volume is located at ρ=0.7-0.8. Here we call turbulence measured by 2D-PCI "low k turbulence" and by high k BS "high k turbulence". Presently, the turbulence amplitudes measured by PCI and high k BS are not absolutely calibrated. Thus, comparisons between low k turbulence measured by PCI and high k turbulence measured by high k BS are not possible. Comparisons are possible for each diagnostics between low and high density cases.

Turbulence measured by 2D-PCI and high k BS show clearly different responses. As shown in Fig.1 (a-3), in low density cases, low k turbulence measured by 2D-PCI shows higher amplitude in D plasma than in H plasma. On the other hand, high k turbulence measured by high k BS shows almost the same turbulence amplitude. On the other hand, in high density cases, as shown in Fig.1 (b-3) and (b-4), low k turbulence measured by 2D-PCI shows clear reduction, while high k turbulence measured by high k BS shows clear increase of the turbulence. The isotope effects of the turbulence are different in low k region (ion scale) and in high k region (electron scale). In the following section, 2D-PCI are used for the investigation of the isotope effects because 2D-PCI can provide turbulence spatial profile of almost the entire region.

2.2 Comparison of profiles in H and D plasma

In this section, profiles of H and D plasma in low and high density of Fig.1 are shown in detail for the investigation of the isotope effects. Profiles of n_e were measured by multi-channel FIR laser interferometer [17], Profiles of T_e by YAG Thomson scattering[18] and Ti profiles by charge exchange spectroscopy[19]. The profiles of n_e and T_e were accumulated for 0.5 sec steady state in Fig.1 in order to reduce the statistical error. Profiles of T_i are obtained by accumulation over one or two beam blips with 20msec exposure time during the 0.5sec steady state. Plasma pressure profiles were estimated from n_e, T_e, and T_i profiles. The spatial profiles of turbulence amplitudes were measured by 2D-PCI [14,15] for 0.5sec steady state and normalized by density profiles. Then, spatial profiles of turbulence level ($\tilde{n}_e/n_e$) are shown. Power balance analyses were carried out by using TASK3D [20] and neoclassical coefficients were estimated by GSRAKE [21]. In the following analyses, the typical uncertainty of χ_e and χ_i is about 10~30%. This is due to the error in the profile measurements.

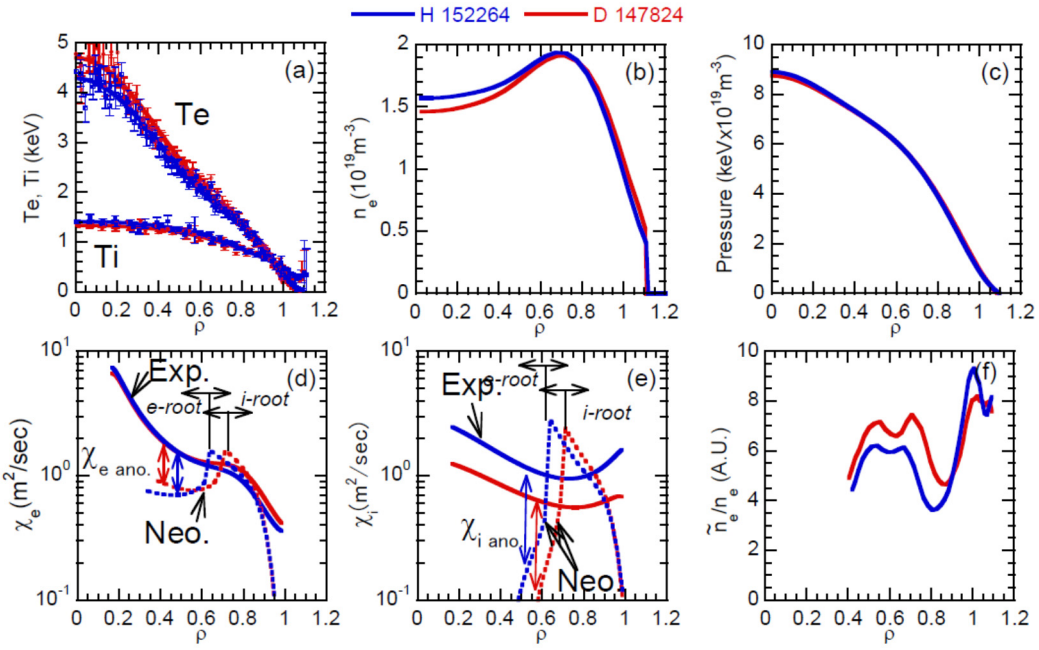

FIG.2 Profiles in low density (a) T_e,,T_i, (b) n_e, (c) pressure, (d) χ_e, (e) χ_i, and (f) turbulence level In (d) and (e), χ_e, and χ_i from power balance analyses are shown by plain line, from neoclassical estimations are shown by dashed line

Figure 2 shows comparisons of profiles in low density case. At $\rho < 0.8$, T_e is slightly higher in D plasma, however n_e is slightly lower in D plasma. Then, kinetic pressure is almost identical suggesting that kinetic energy confinement time is comparable. There is small difference from diamagnetic τ_E, which is 5% better in D plasma.

As shown in Fig2 (d) and (e), the experimental value of χ_e is almost identical in H and D plasma. On the other hand, experimental χ_i is lower in D plasma over the entire region. In ECRH plasma, the only ion heating mechanism is equipartition by energy transfer from electrons to ions. The electron-ion equipartition heating power (P_{ei}) is inversely proportional to ion mass for same density and temperature difference [22]. Thus, P_{ei} in D plasma is almost one-half of P_{ei} in H plasma. However, achieved T_i is almost identical. Consequently, experimental χ_i in D plasma becomes about half that of H plasma.

In Fig.2 (d) and (e), neoclassical χ_e and χ_i are shown by dashed lines. The difference between experimental and neoclassical χ_e, χ_i are anomalous contribution ($\chi_{e\ ano}$, $\chi_{i\ ano}$). These are almost identical both in H and D plasma.

The following should be noted regarding neoclassical transport. In neoclassical transport, neoclassical ambipolar condition determines neoclassical electron root (e-root) and ion root (i-root). Neoclassical e-root is formed with positive Er and reduces neoclassical transport coefficients. Neoclassical e-root is obtained at high T_e/T_i[23,24]. On the other hand, neoclassical i-root is formed with negative Er and enhances neoclassical transport coefficients at low T_e/T_i[25]. In low density

cases, neoclassical e-root is found at $\rho < 0.6$ in H plasma and $\rho < 0.7$ in D plasma. On the other hand, neoclassical i-root is found at $\rho > 0.6$ in H plasma and $\rho > 0.7$ in D plasma. At around transition position between e-root and i-root, neoclassical χ_e and χ_i exceed experimental values. These estimations are physically unacceptable and are overestimated. Present estimation using GSRAKE for LHD plasma neglects the contribution of magnetic drift to poloidal precession of trapped particles. This simplification results in overestimation of the neoclassical radial transport in ion root with weak ExB rotation[26]. Global calculation taking into account the full drift motion should be performed for the more precise estimation, although large computation time is required.

The isotope effects on neoclassical transport were reported in ref. 27. Isotope effects are weak in electron root and negligible in ion root. The small differences in neoclassical χ_e and χ_i in Fig.2 (d) and (e) are not due to the isotope effects but due to the small difference of the plasma profile.

Figure 2 (f) shows comparison of turbulence level obtained using 2D-PCI. The shape of the profile is similar. There are two peaks, which are at ρ =0.6 and 1.0, respectively. Turbulence level is higher at $\rho < 0.8$ in D plasma and comparable at $\rho > 0.8$ in H and D plasma.

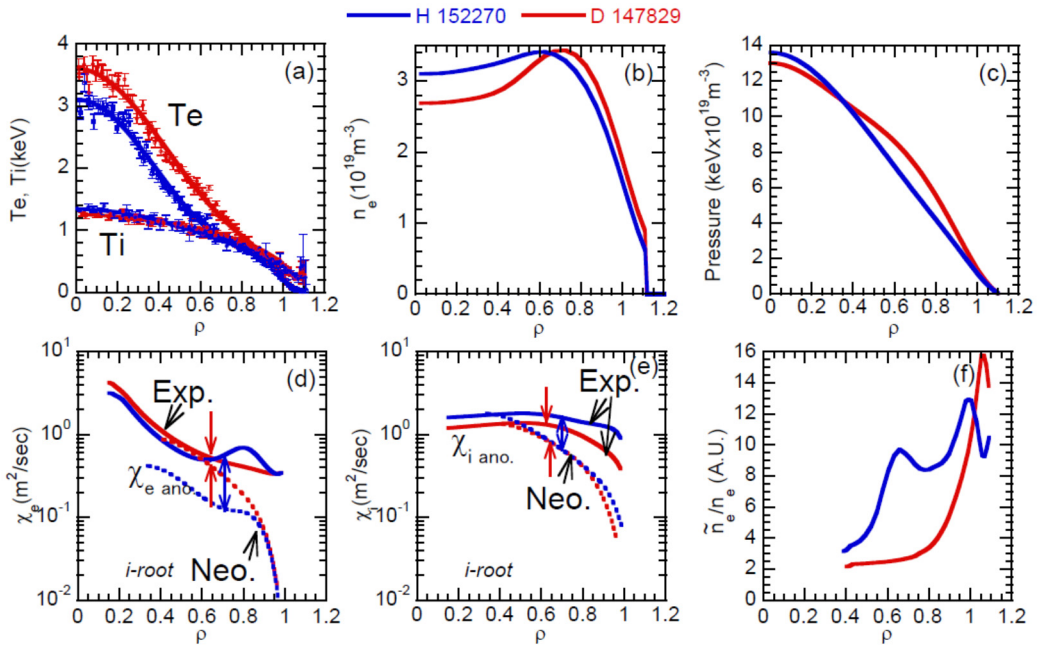

FIG.3 Profiles in high density (a) T_e,,T_i, (b) n_e, (c) pressure, (d) χ_e, (e) χ_i, and (f) turbulence level In (d) and (e), χ_e, and χ_i from power balance analyses are shown by plain line, from neoclassical estimations are shown by dashed line

Figure 3 shows profiles in high density cases. Many profiles are clearly different in H and D plasmas except T_i profiles. As shown in Fig.3 (a), T_i profiles are almost identical in H and D plasma. However, T_e profiles are clearly higher in D plasma than in H. It should be noted that the difference is clear at $\rho<0.8$. As shown in Fig.3 (b), density profiles are also clearly different at $\rho<0.8$. The

density profiles are more hollow in D plasma. According to ref.11, this is not due to the difference of neutral penetration of H and D, nor is it due to the difference of impurity profiles.

As shown in Fig. 3 (c), kinetic pressure profiles are also clearly different. The kinetic pressure is lower in D plasma at $\rho<0.4$, but is higher in D plasma at $\rho>0.4$. Thus, volume integrated kinetic pressure is clearly higher in D plasma. This corresponds to the 15% better diamagnetic τ_E in D plasma.

As shown in Fig.3 (c), χ_e is comparable at $\rho < 0.6$ but lower in D plasma at $\rho = 0.6 \sim 0.9$. However, neoclassical χ_e is clearly higher in D plasma at $\rho < 0.9$. In high density case, entire region is neoclassical i-root. Thus, there are no isotope effects in neoclassical transport. The higher neoclassical contribution to χ_e in D plasma is not directly related to the ion species but due to the higher T_e. Therefore, the anomalous contribution to χ_e ($\chi_{e\,ano}$) is clearly reduced in D plasma.

As shown in Fig. 3 (d), experimental χ_i is lower in D plasma as well as in low density cases. This is due to the lower P_{ei} in D plasma and almost identical T_i profiles in H and D plasmas. Neoclassical χ_i is almost identical. The anomalous contribution of χ_i ($\chi_{I\,ano}$) is lower in D plasma.

As shown in Fig. 3 (e), turbulence level from 2D PCI is clearly different both in profile shape and quantities. The turbulence level is clearly lower at $\rho<0.9$, where $\chi_{e\,ano}$ is clearly reduced in D plasma. Detailed differences of turbulence characteristics are described in the next section.

2.3 Comparison of turbulence characteristics

In this section, detailed characteristics of the low-k turbulence measured by 2D-PCI are described. Figure 4 and 5 show comparison of spatial profiles of turbulence amplitude, wavenumber spectrum and phase velocity in low and high density cases respectively. In Fig. 2 and 3, turbulence levels ($\tilde{n}_e/n_e$) are shown. However, in this section, turbulence amplitude without normalization is shown. The turbulence level should be used to compare different background density. However, turbulence level includes uncertainty of the density profile and spatial position of the turbulence. On the other hand, turbulence amplitude is the directly measured quantity by 2D-PCI. Thus, turbulence amplitude is preferable for arguing detailed characteristics. The 2D-PCI measured turbulence from lower and upper side of equatorial plane[11]. Sometimes, up-down asymmetry is seen [28,29]. This is likely due to the formation of turbulence eddy tilting [15, 30], however, in this dataset the measured turbulence was almost symmetric at lower and upper side of the plasma. Thus, profiles in only upper side of measured location ($\rho >0.4$) are shown.

Figure 4 shows turbulence profiles in low density case. As shown in Fig.5 (a-1) and (b-1), the turbulence amplitude is higher in D plasma. Thus, turbulence level ($\tilde{n}_e/n_e$) is also higher in D plasma under almost identical n_e profile. Two different components are clearly seen. One exists at $\rho = 0.4 \sim 0.8$ and the other exists at $\rho = 0.8 \sim 1.1$. For this purpose, the region $\rho = 0.4 \sim 0.8$ is referred to the core, whilst $\rho = 0.6 \sim 1.1$ is referred to as the edge.As shown in Fig. 4 (a-2) and (b-2),

the measured peak wavenumber is not significantly different between H and D plasma, being around 0.3 mm^{-1} in both the core and edge regions.

As shown in Fig. 4 (a-3) and (b-3), core turbulence propagates towards the ion diamagnetic direction in the laboratory frame both in H and D plasma. On the other hand, edge turbulence propagates towards the electron diamagnetic direction in the laboratory frame both in H and D plasma. These phase velocities follow rotation velocities (V_{EXB}), which were measured by charge exchange spectroscopy (CXRS). It is difficult to distinguish the propagation direction in the plasma frame within the experimental accuracy.

In the low density case, shown in Fig. 4 (a-1) and (b-1), the spatial structure is similar both in H and D plasma. The amplitude is higher in D plasma.

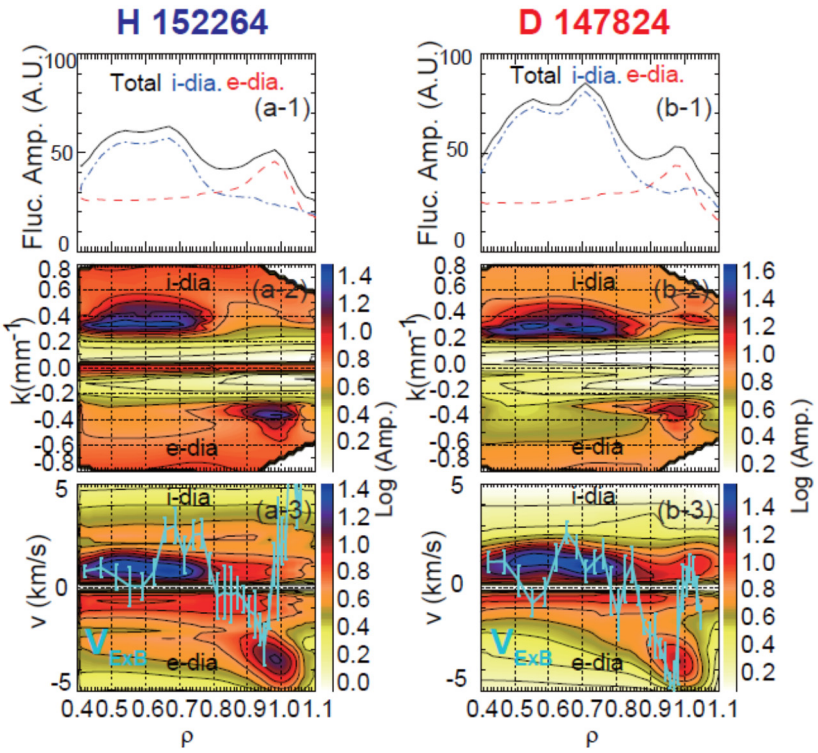

FIG.4 Spatial profiles of low density case (a-1), (b-1) turbulence amplitude, (a-2), (b-2) wavenumber spectrum and (a-3), (b-3) turbulence phase velocity
In (a-3) and (b-3), V_{EXB} measured by CXRS are shown by blue line.

In the high density case, shown in Fig. 5 (a-1) and (b-1), both spatial structure and amplitude are clearly different in H and D plasma. In H plasma, turbulence exists over the entire measurable region of ρ = 0.4 - 1.1. On the other hand, in D plasma dominant components exist in the edge region (ρ >0.8) only. Clear difference of turbulence amplitude results in clear difference of turbulence level as shown in Fig.3. (f).

As shown in Fig.5 (a-2), (b-2), the dominant k is 0.3mm^{-1} both in H and D plasma. As shown in Fig.5 (a-3), in H plasma, only electron diamagnetic propagation component exists. On the other hand, as shown in Fig.5 (b-3), in D plasma, the component at $\rho < 1.0$ is propagating toward the electron diamagnetic direction and the components at $\rho > 1.0$ propagate ion diamagnetic direction. As shown in Fig.5 (a-3), in H plasma, phase velocity at $\rho = 0.6 \sim 0.8$ deviates from V_{EXB} suggesting that the propagation direction of the turbulence is in the electron diamagnetic direction in plasma frame. On the other hand, as shown in Fig. 5 (b-3), phase velocity of the turbulence in D plasma follows V_{EXB}.

It should be emphasized that clear difference of turbulence characteristics were observed in high density case between H and D plasma, where T_e and n_e profiles are clearly different under identical line averaged density and heating conditions. Thus, the observed difference of the turbulence in high density cases is key to the understanding of isotope effects.

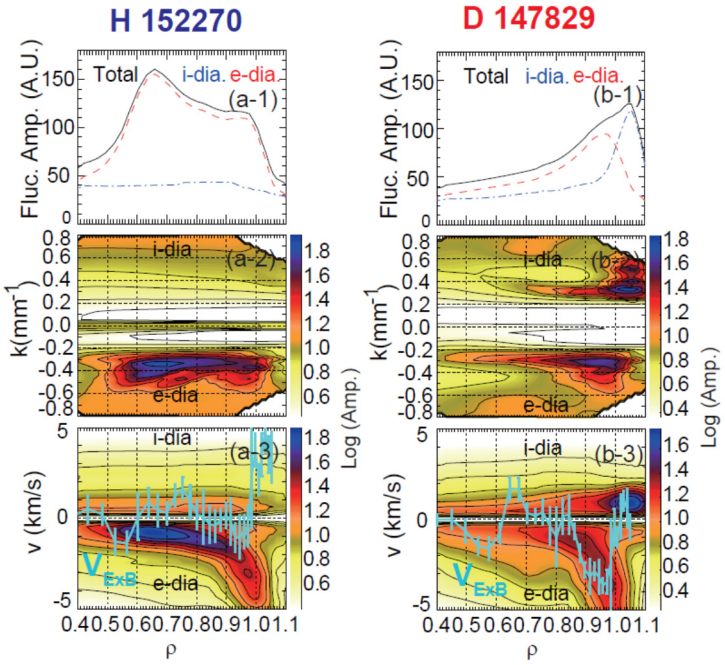

FIG.5 Spatial profiles of high density case (a-1), (b-1) turbulence amplitude, (a-2), (b-2) wavenumber spectrum and (a-3), (b-3) turbulence phase velocity
In (a-3) and (b-3), V_{EXB} measured by CXRS are shown by blue line.

2.4 Gyrokinetic linear analyses

For the detailed arguments regarding turbulence characteristics, gyrokinetic linear analyses were performed. Analyses were carried out at ρ =0.5 and 0.7, where differences of profiles were seen in high density case. Local flux tube gyrokinetic code (GKV [31]) were used for the analyses. Both kinetic ions and electrons were included in the the stability analyses. Only a single ion species was included in these calculations -- Hydrogen for H plasma and Deuterium for D plasma; impurity ions

were not included. Electrostatic assumption was made for the calculation runs, and collisionality effects were included. However, the effects of ExB shearing were not included in these analyses. As shown in Fig. 4 (a-3), (b-3) and Fig. 5 (a-3), (b-3), there are fine structures of V_{EXB} at ρ =0.5 ~ 0.7, but these are likely to be an experimental uncertainty. On the other hand, turbulence phase velocity, which shows V_{EXB} approximately, stays almost constant in space. Because of these observations, effects of ExB shearing rate were neglected.

Figure 6 shows analysis results for ρ=0.5 and ρ=0.8 in both high density and low density cases, comparing H and D plasmas. Input parameters are shown in table. 1. Magnetic parameters are almost identical in the calculation. Horizontal axis is normalized wavenumber $k_y\rho_I$, with k_y being the poloidal wavenumber. The ion Larmor radius was calculated for Hydrogen and Deuterium, respectively. The dimension of growth rate and real frequency are kHz unit in order to compare their absolute values in H and D plasma. Calculations were performed at $k\rho_i$ = 0.05 ~ 1.0 every 0.05 step at $k\rho_i$ = 1 ~ 20 every 1 step. Only unstable solutions were shown in Fig.6. In Fig.6, measured normalized wavenumber $k\rho_i$ are shown by arrows. Although the measured peak k was almost identical at around 0.3mm^{-1} by PCI, ρ_i becomes larger in D plasma at almost identical T_i. Then, the measured $k\rho_i$ becomes approximately factor 1.4, which is square root of H and D mass ratio, larger in D plasma.

In the low k region ($k\rho_i$ <~ 1), the dominant mode is ITG, In the previous analyses of LHD ECRH plasma, TEM was found to be unstable at ρ = 0.3, $n_{e\,bar}$=0.8x10^{19}m^{-3} [32]. In Fig.2 of ref.32, the $n_{e\,bar}$ is lower and T_e is higher than ones in the present analyses. Also, at this location (ρ = 0.3) in Fig.2 of ref.32, T_i gradient is very flat. Thus, electron temperature driven TEM can be unstable.

On the other hand, at the positions analyzed in this section (ρ =0.5 and 0.7), normalized T_i gradient (-grad T_i/T_i) is large enough to destabilize ITG. Then, the normalized density gradient (-grad n_e/n_e) and T_e/T_i also plays a role on stability. The reduction of the normalized density gradient reduces the growth rate [32]. This tendency continues after the sign of the gradient changes from positive to negative. In other words, the more hollow density profile stabilizes ITG turbulence [32]. For all cases in Fig.6, growth rates are lower in D plasma in low k region. The ruling parameters are likely to be normalized n_e and T_i gradient and T_e/T_i. Without collisionality effects, both ITG and TEM have a gyro-Bohm scaling, where growth rate is proportional to square root of ion mass, so that the growth rate is higher in D plasma under these condition. Including collisionality effects, however, TEM has anti gyro-Bohm characteristics, where the growth rate becomes lower in D plasma, whilst ITG keeps gyro-Bohm characteristics [33]. Furthermore, TEM is more strongly stabilized by collisionality effects in D plasma than in H plasma [33]. The difference of the collisionality stabilization effects are apparent in TEM. However, dominant mode is ITG, thus, the reduced ITG growth rate in D plasma is not due to the collisionality stabilization for Hydrogen and Deuterium but due to the difference of profile. The collisionality stabilization effects are negligible in ETG.

Thus, the difference of ETG growth rate is also due to the difference of profiles.

Figure 6 (a), (c) shows the linear spectrum in low density cases. In low density cases, anomalous components of electron and ion transports are almost comparable in H and D plasma as shown in Fig.2 (d) and (e). Turbulence level is higher in D plasma as shown in Fig.2 (f). Spatial structure and wavenumber spectrum are similar in H and D plasma as shown in Fig. 4. Linear analyses show reduced growth rate in D plasma. Entire unstable regions of low k region are ITG. The reduced growth rates in D plasma are due to more negative normalized n_e gradient and lower normalized T_i gradient both at $\rho = 0.5$ an 0.7 as listed in table 1.. The ITG growth rate is lower at $\rho = 0.7$ than at $\rho = 0.5$, although both n_e and T_i gradients are steeper at $\rho = 0.7$ than at $\rho = 0.5$. This is because T_e/T_i is lower at $\rho = 0.5$ than at $\rho = 0.7$.

At $\rho = 0.5$ in low density case, ETG growth rate is much higher than ITG growth rate. However, this does not indicates ETG plays more significant role on transport than ITG. ETG contribute the transport, when streamer structure is formed [34]. Non linear simulation is necessary for the investigation of streamer. As shown in Fig.1 (a-4), turbulence signal is clear in ETG region. However, as shown in Fig. 6(c), ETG region is stable. Further investigations are necessary for ETG turbulence. In low density cases, anomalous transport is comparable in H and D plasma, turbulence level is higher in D plasma and linear growth rate is lower in D plasma. The correspondences among three quantities are not clear.

Figure 6 (c) and (d) show linear spectrum in high density cases. In high density cases, anomalous component of electron and ion transports are reduced in D plasma as shown in Fig.3 (d) and (e). Turbulence level from PCI is lower in D plasma as shown in Fig.3 (f). Spatial structures of turbulence are clearly different in H and D plasma and as shown in Fig. 5.

In high density cases, as shown in Fig. 6 (b) and (d), the growth rate of low k region is lower in D plasma at $\rho = 0.5$ and 0.7. At $\rho = 0.7$, the growth rate for all calculated $k\rho_i$ is stable (negative). As shown in table 1, at $\rho=0.5$, normalized n_e gradient is lower (more negative) and normalized T_i gradient is lower in D plasma than in H plasma. The value of T_e/T_i is higher in D plasma. Higher T_e/T_i makes ITG/TEM more unstable. However, at both $\rho=0.5$ and $\rho=0.7$ in high density cases, the lower normalized n_e and T_i gradients play a more significant role, leading to the growth rate being lower in D plasma than in H plasma.

In high density case, as shown in Fig. 6 (b) and (d), high k region is unstable at $\rho = 0.5$ and 0.7 both in H and D plasma. At $\rho = 0.5$, as shown in Table 1, R/L_{Te} and R/L_n are lower and T_e/T_i is higher in D plasma than in H plasma, these result in lower ETG growth rate in D plasma. On the other hand, at $\rho=0.7$, lower R/Ln and higher Te/Ti in D plasma than in H plasma reducing ETG growth rate in D plasma is canceled out by higher R/Lte in D plasma increasing ETG growth rated. Then, growth rate is comparable in D and H plasma.

In high density cases, anomalous transport is lower in D plasma, turbulence level from PCI is lower

in D plasma and linear growth rate of low k region is lower in D plasma. The correspondences among three quantities are clear. However, there is one contradiction. In high density H plasma, the measurement shows that turbulence propagates toward the electron diamagnetic direction in plasma frame. This is against characteristics of ITG, of which propagation direction is ion diamagnetic direction. Further detailed experimental confirmation is necessary.

The gyrokinetic linear investigation shown in this section is the first step study using experimental profile. The result of linear run is very sensitive to input parameter. The T_i profiles are very similar as shown in Fig2 (a) and Fig.3(a). However, the normalized T_i gradient is slightly lower in D plasma. Such small difference affects gyrokinetic results significantly. In the next step, investigation of the sensitivity of input parameter should be performed. Then, nonlinear run will be performed for the quantitative investigation of turbulence driven transport. Also, non linear run is important in order to investigate the role of ETG turbulence.

In other devices, there are reports of TEM in ECRH plasma of stellarator/heliotron. In ATF, dissipative TEM is reported by microwave scattering measurements and analytical investigation of turbulence mode were performed [35]. In HSX, core turbulence measured by interferometer suggested temperature gradient driven TEM [36]. Recently, in TJ-II, Doppler reflectmetry measurements showed the measured turbulence was TEM from the comparison with gyrokinetic linear analyses [37]. In these devices, due to the lower heating power than LHD, T_i gradients are very flat, then, TEM can be unstable.

ion	shot	density	ρ	R/Ln	R/Lte	R/Lti	Te/Ti	ITG	ETG
H	152264	low	0.5	-3.85	11.87	3.97	2.02	unstable	unstable
H	152264	low	0.7	0.41	12.6	8.53	1.59	unstable	stable
D	147824	low	0.5	-4.45	12.56	3.6	2.20	unstable	unstable
D	147824	low	0.7	-0.36	13.12	7.66	1.76	unstable	stable
H	152270	high	0.5	-1.49	16.54	5.69	1.39	unstable	unstable
H	152270	high	0.7	2.91	13.44	8.31	1.05	unstable	unstable
D	147829	high	0.5	-4.49	13.66	3.58	1.90	unstable	unstable
D	147829	high	0.7	-0.68	16.7	6.05	1.34	stable	unstable

Table 1 Input parameters of gyrokinetic linear analyses

$L_n^{-1}=1/n_e\ dn_e/d\rho$, $L_{Ti}^{-1}=1/T_e\ dT_e/d\rho$, $L_{Ti}^{-1}=1/Ti\ dT_i/d\rho$, R is major radius.

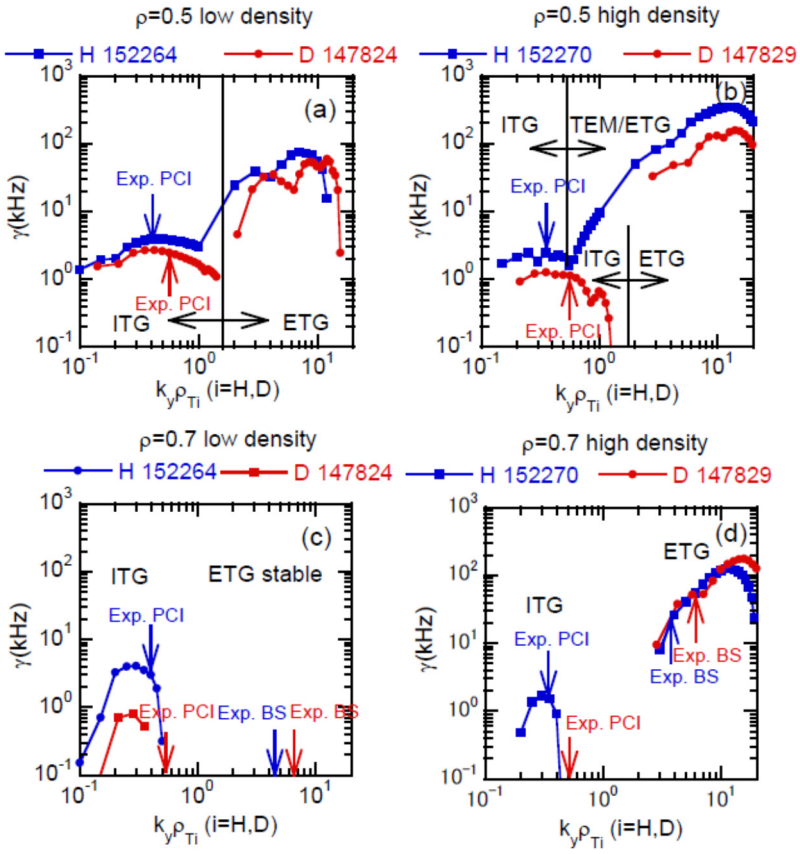

FIG.6 Linear spectrum of growth rate (γ)at ρ=0.5 and ρ=0. 7
(a) ~ (b) low density case (H 152264, D 147824) and (c),(d) high density case (H 152270, D 147829) $k_y\rho_i$ is the normalized wavenumber, where ρ_i is ion Larmor radius. ρ_i is calculated for hydrogen and deuterium ion mass respectively. The measured $k_y\rho_i$ are shown by arrow.

2.5 Parameter dependence of isotope effect

In this section, the parameter dependence of transport coefficients and turbulence level is discussed. The experimental and neoclassical χ_e, χ_i, and turbulence level are averaged over ρ = 0.5 - 0.8, where a clear difference of transport and turbulence between H and D is observed in high density cases. In a previous study [11], such surveys were already performed. However, the survey for the χ_e and χ_i did not include high density data, which shows clear reductions of $\chi_{e\,ano}$ and $\chi_{i\,ano}$. The survey of the turbulence level included different heating condition. In this study, the data set in H and D plasma are obtained under almost identical heating conditions (~2MW 154GHz 2nd harmonic ECRH, ρ = 0.1 deposition). The density was scanned from 1x10^{19}m^{-3} ~ 3x10^{19}m^{-3} by changing gas fueling. A scan of the density with identical heating power results in the scan of collisionality of one order magnitude. With use of 154GHz, refraction effects are almost negligible. The more than 80% power was deposited at ρ = 0.1.

Firstly, collisionality dependence of experimental and neoclassical χ_e and χ_i are discussed. Then, the driving term and the stabilizing term of turbulence are discussed. The collisionality affects both

neoclassical and anomalous transport. Whilst experiments were performed by scanning density, the key parameter of interest is the collisionality. More particularly, characteristics of the transport are determined by three dimensionless parameters, which are normalized collisionality (ν*), normalized ion Larmor radius (ρ*), and normalized pressure (β). Among three non-dimensional parameters, ν* is most widely scanned in the present dataset. Thus, dependence of χ_e, χ_i and turbulence level are investigated for collisionality. The normalized collisionality in this report is defined as $\nu^*_h = \nu_{ei}/(\varepsilon_{eff}^{3/2}\nu_T/qR_{mj})$. ν_{ei} is the electron ion collision frequency, ν_T is the electron thermal velocity, q is the safety factor, R_{mj} is the major radius, and ε_{eff} is an effective helical ripple [38, 39]. $\nu_h^* = 1$ is the boundary between 1/ν, where neoclassical coefficients are inversely proportional to collisionality, and plateau regime. However, it should be noted that neoclassical transport is also affected by different ambipolar conditions such as e-root and i-root as described in Sec.2.2. With increase of ν_h^* by the increase of density, T_e/T_i decreases. Whilst e-root is present at higher T_e/T_i, there is a transition to i-root as T_e/T_i decreases.

Figure 7 (a) shows the ν_h^* dependence of experimental and neoclassical χ_e. Both experimental and neoclassical χ_e reduce with increase of ν_h^*. GSRAKE show e-root at $\nu_h^* < 1.4$ and i-root at $\nu_h^* > 1.4$. At around transition ν_h^* between e-root and i-root, neoclassical χ_e approached to experimental χ_e. At $\nu_h^* > 1.4$, neoclassical χ_e decreases at a faster rate than experimental χ_e. Then, anomalous χ_e, which is difference between experimental and neoclassical χ_e, increases with ν_h^*. At $\nu_h^* < 2$, both experimental and neoclassical ν_h^* does not show a clear difference between H and D plasma. This is the same as previous results [11]. At $\nu_h^* > 3$, although only one single data point is available in D plasma, experimental χ_e is lower in D plasma than in H plasma. Also, anomalous χ_e, which is the difference between the experimental and neoclassical values of χ_e as shown by arrows in Fig. 7 (a), are clearly smaller in D plasma than in H plasma. This indicates that anomalous electron transport is reduced in D plasma at higher ν_h^*.

Figure 7 (b) shows the ν_h^* dependence of χ_i. Both experimental and neoclassical χ_i increase with ν_h^*. The equipartition heating to ion increases with increase of ν_h^*. T_i increases at higher density as shown in Fig.2 (a) and Fig.3 (a). Thus, experimental χ_i increases due to the power degradation with increase of ν_h^*. Neoclassical χ_i increases due to the increase of T_i with ν_h^*. Experimental χ_i is lower in D plasma than in H plasma. This is because P_{ei} is lower in D plasma and almost identical T_i was obtained as described in Sec.2.2. Neoclassical χ_i is comparable with experimental χ_i. As shown in Fig. 2 (e), at some locations, neoclassical χ_i exceeds experimental χ_i. As described in Sec. 2.2, neoclassical coefficients are likely to be overestimated due to the local calculation. Presently, it is difficult to judge if ion transport is at the neoclassical level or not. Detailed analyses using global neoclassical calculations are necessary.

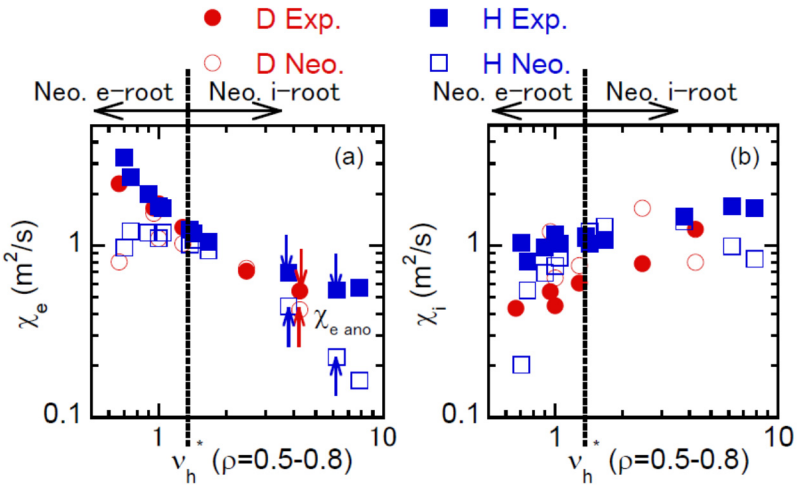

FIG.7 Collisionality dependence of (a) $\chi_{e\,exp}$, $\chi_{e\,neo}$ and (b) $\chi_{i\,exp}$, $\chi_{i\,neo}$

Theoretical investigation by gyrokinetic linear analyses are described in Sec.2.4. In this section, driving terms of the turbulence are discussed from the experimental data. Figure 8 shows the ν_h^* dependence of turbulence level, as well as normalized gradient of n_e, T_e, T_i, and plasma pressure (P). Both turbulence level and normalized gradients were averaged at $\rho = 0.5 - 0.8$. Data set is the same discharge and analysis timing as those in Fig. 7, which was density scan with identical ECRH (~2MW $\rho = 0.1$ deposition).

Two important characteristics are seen in Fig.8 (a). Firstly, turbulence level is higher in D plasma than in H plasma at $\nu_h^*<1.4$, but turbulence level is lower in D plasma than in H plasma at $\nu_h^* >4$. Secondly, in H plasma, turbulence level decreases with increase of the ν_h^* at $\nu_h^* < 4$, however, the turbulence level increases at $\nu_h^* >4$. In a separate dataset of D plasma [11], which includes different heating conditions, the turbulence level at $\nu_h^* >4$ increased as well. The normalized n_e and P gradient decrease as ν_h^* increases at $\nu_h^*< 3$, then they both increase with ν_h^* at $\nu_h^*>3$ as shown in Fig. 8 (a). The ν_h^* dependence of normalized n_e and P gradients is similar to the ν_h^* dependence of turbulence level as shown in Fig. 8 (e). These observations show that both normalized n_e and P gradient play a role on turbulence level.

At ν_h^* ~4, where turbulence level is clearly lower in D plasma than in H plasma, the normalized gradient of n_e, T_i, and P are lower in D plasma but T_e gradient is higher in D plasma than in H plasma. These results suggest that normalized gradients of n_e, T_i and P may also play a role in controlling the turbulence level, in addition to any such isotope dependence.

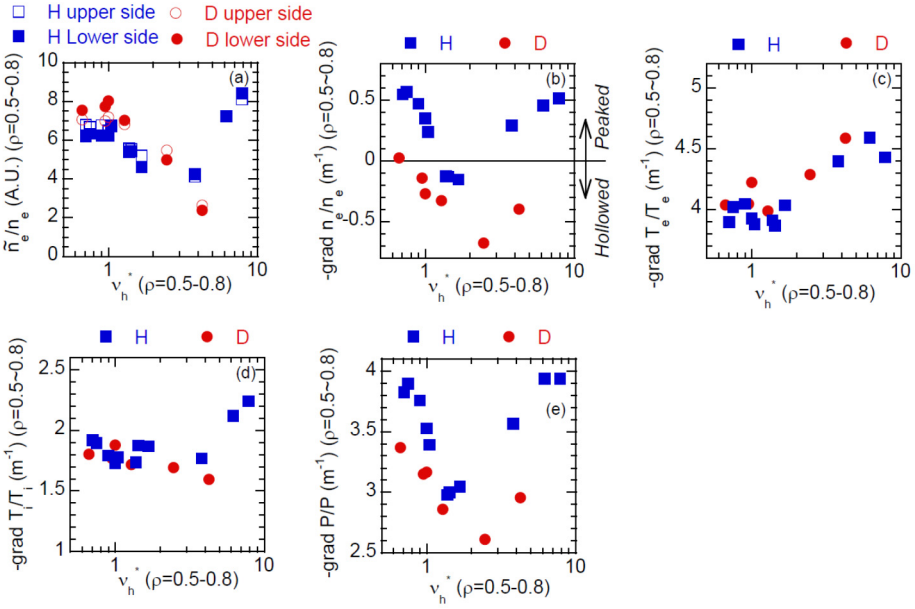

FIG.8 Collisionality dependence of core (ρ=0.5-0.8) (a) turbulence level from PCI, normalized gradient of (b) density, (c) electron temperature, (d) ion temperature, and (e) pressure

Figure 9 shows collisionality dependence of turbulence level from high k BS. The measurements location is ρ =0.7-0.8. Thus, turbulence level was estimated from the ration of measured turbulence and averaged density at ρ = 0.7-0.8. The turbulence level reduces with increase of collisionality at $\nu_h^* < 2$, then, turbulence level is almost constant at $\nu_h^* > 2$. The collisionality dependence is different from the one of low k turbulence measured by PCI (Fig.8 (a)). In Hydrogen plasma, turbulence level cincrease at $\nu_h^*>4$ as shown in Fig.8 (a), however, but, increase of the turbulence level with increase of the collisionality are not clear in high k turbulence. These observations indicate that characteristics of low k and high k turbulence are different.

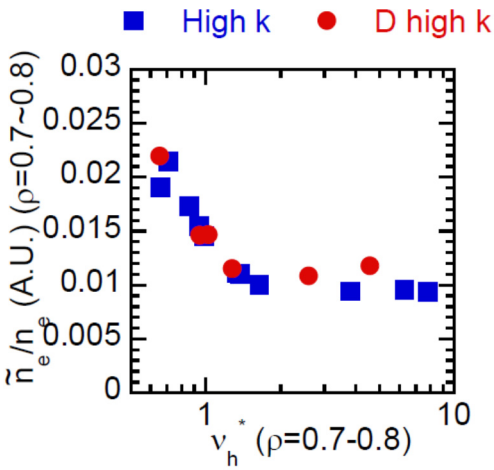

FIG9 Collisionality dependence of turbulence level from high k BS

3. Investigation of isotope effects on particle transport

The results described in Sec. 2 suggest the importance of the particle transport in the isotope effects. In this section, the results of density modulation experiments in H and D plasma are described. Density modulation experiments are a powerful experimental scheme for the qualitative estimation of transport coefficients. The first density modulation experiments were performed in TEXT tokamak [40]. There are two advantages in this technique. Firstly, it is possible to estimate diffusion coefficients and convection velocity separately. Secondly, the absolute value of particle source, which is technically difficult to estimate, is not necessary. Only relative shape, which is available from the Monte Carlo simulation of neutral penetration, is necessary. However, interpretation of the coefficients must be careful. If there is a non linearity between normalized particle flux and normalized density gradient, diffusion coefficients and convection velocities from modulation experiments can be different ones in equilibrium state [41]. In LHD, systematic experiments of density modulation experiments were performed in normal confinement NBI heated plasma [44]. The results in ref. 44 show that density profile becomes hollower at lower ν_h^* and more outwardly shifted configuration, where neoclassical transport becomes significant. Then, diffusion coefficients are anomalous and convection velocities are close to neoclassical convection velocity, which are mainly due to neoclassical thermo-diffusion.

Investigations of isotope effects by density modulation have been carried out in both tokamaks and stellarators/heliotrons alike. In ASDEX ohmic discharge, lower diffusion and lower inward pinch in D plasma than in H plasma were reported [43]. In CHS NBI heated plasma, in the low density regime (line averaged density $< 2.5 \times 10^{19}$ m^{-3}), the lower particle diffusivity and the larger inwardly directed core convection velocity was observed in the deuterium dominant plasma, while in the high density regime (line averaged density $>2.5 \times 10^{19}$ m^{-3}) no clear difference was observed [44]. In Heliotron-J ECRH plasma, lower modulation frequency (50Hz) showed reduced diffusion coefficients and reduced convection velocities, while higher modulation (100 and 125Hz) did not show clear differences[45].

Recently, a new analysis technique is developed [46]. In past analyses in LHD, four fitting variables (two for diffusion coefficients and two for convection velocities) were used. Then, fitting was performed to modulation profile and equilibrium profile simultaneously. In the new technique, at first radial profile of modulation amplitudes are estimated from the Abel inversion of the 10ch FIR laser interferometer data. Then, diffusion coefficients and convection velocities fit directly to those profiles. Diffusion coefficients and convection velocities are expressed by 27 fitting variables each for diffusion coefficients and convection velocities. Fitting was performed only for the modulation components. Therefore, estimated diffusion coefficient and convection velocity were defined as D_{mod} and V_{mod} in order to discriminate the diffusion coefficients and convection velocities in equilibrium state (D_{eq} and V_{eq}). In order to make the convergence of the fitting possible, generic algorithm (GA)

quasi newton (QN) method were used [46]. Relative shape of particle source rate was estimated by EIRINE code [47].

For the density modulation experiments, longer duration of plasma is preferred to have large number of modulation periods. Thus, each gyrotron power was reduced down to ~0.5MW. Two 154GHz second harmonic resonant heating and one 77GHz fundamental resonant heating were used. Total heating power was ~1.5MW. The deposition location was ρ = 0-0.1.

Figure 10 shows time trace of modulation experiments in low density ($n_{e\,bar}$~$1.6x10^{19}m^{-3}$) and high density ($n_{e\,bar}$~$2.6x10^{19}m^{-3}$). Figure 10 shows similar characteristics to ones in Fig.1. In low density cases, central T_e was almost identical in H and D plasma, while in high density cases, central T_e is higher in D plasma than in H plasma. Modulation frequency was selected to be 2.5Hz. Higher than 2.5Hz, Abel inversion of modulation components became difficult in the present dataset.

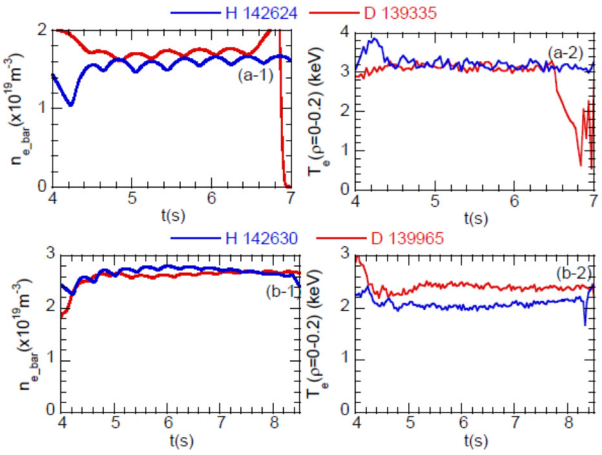

FIG.10 Time history of density modulation experiments in low density (a-1) $n_{e\,bar}$, (a-2) T_e(ρ = 0-0.2) and in high density (b-1) $n_{e\,bar}$, (b-2) T_e(ρ = 0-0.2)

Figure 11 shows the results of density modulation experiments in low density cases. As shown in Fig.11, (a), (b), both background n_e and T_e profiles show small difference. This is similar to the low density cases shown in Fig. 2. However, as shown in Fig.11 (c) and (d), modulation amplitude is clearly different. Figure 11 (e) and (d) shows D_{mod}, V_{mod}, and neoclassical coefficients (D_{neo}, V_{neo}.). The neoclassical particle flux is shown by the following equation [20].

$$\Gamma_{e\_neo} = -n_e D_1 \left\{ \frac{\nabla n_e}{n_e} + \frac{eE_r}{T_e} + \left(\frac{D_2}{D_1} - \frac{3}{2} \right) \frac{\nabla T_e}{T_e} \right\} \quad (1)$$

Then, neoclassical convection velocities are shown by the following equation.

$$V_{e\_neo} = -D_1 \left\{ \frac{eE_r}{T_e} + \left(\frac{D_2}{D_1} - \frac{3}{2} \right) \frac{\nabla T_e}{T_e} \right\} \quad (2)$$

At ρ = 0.8, D_{mod} has its minimum value, and so the difference between D_{mod} and D_{neo} is also smallest at this location. This may correspond to the minimum of turbulence level observed as shown in Fig.2 (f). D_{mod} is much higher than D_{neo}, at most of the radial locations suggesting that the diffusion process is dominated by the anomalous processes. D_{mod} is lower in D plasma than H plasma for at $\rho < 0.8$ and is comparable between D and H plasmas at $\rho > 0.8$. Fig.11 (f) shows spatial profiles of convection velocity. V_{mod} in H plasma at ρ = 0.6 - 0.8 becomes negative. Present analysis technique is sensitive to spatial profile of modulation amplitude and phase. In particular, shape of the V_{mod} is sometimes ambiguous. The smoothness of the profile of modulation components are numerically optimized by using general cross validation (GCV) technique [46]. However, GCV tends to result in fine profile. More consideration will be necessary to confirm and improve the estimation of D_{mod} and V_{mod}. However, except V_{mod} at ρ = 0.6 - 0.8 in H plasma, V_{mod} are comparable in H and D plasma. Also, V_{mod} are comparable with V_{neo}.

Figure 12 shows results of density modulation experiments in high density cases. As shown in Fig.12 (a) and (b). The n_e profiles are clearly hollower and T_e is clearly higher at $\rho < 0.9$ in D plasma than in H plasma. This observation is similar to other observations in Fig. 3. Modulation amplitude is more localized in the edge region as shown in Fig.12 (c). Modulation phase profiles are clearly different as shown in Fig. 12 (d). As shown in Fig. 12 (e), the difference between D_{mod} and D_{neo} becomes larger in high density cases than the difference in low density cases. This indicates that anomalous contribution becomes larger in high density cases. D_{mod} is slightly lower in D plasma than H plasma at $\rho < 0.8$ and higher in D plasma than H plasma at $\rho > 0.8$ in D plasma than in H plasma. As shown in Fig. 12 (f), V_{mod} in D plasma is negative at $\rho < 0.7$. The values of V_{mod} at $\rho < 1.0$ in H plasma and V_{mod} at ρ = 0.7~1.0 are clearly higher than V_{neo}. However, V_{mod} at ρ = 0.7~1.0 in D plasma is only slightly higher than in H plasma. Values of D_{neo} and V_{neo} are higher in D plasma than in H plasma. This is not due to isotope effects, but due to the higher T_e values in D plasma. The data set of Fig.12 is ion root plasma. As described in Sec.2, there is no istope effects in neoclassical transport in ion root condition.

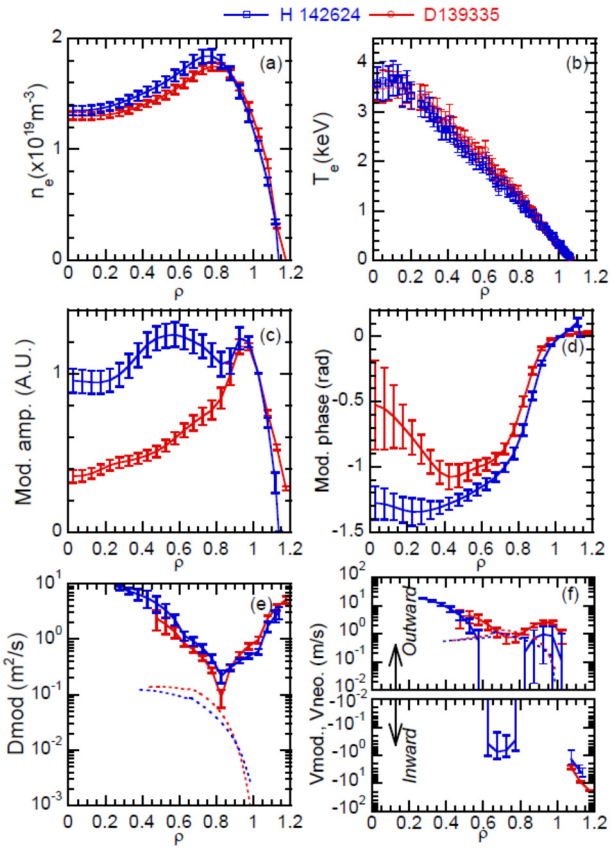

FIG.11 Example of density modulation experiments in low density cases (a) background ne profiles, (b) background T_e profiles (c) modulation amplitude, (d) modulation phase (e) D_{mod}, and (f) V_{mod}. In (e) and (f), plain and dashed lines indicate experimental and neoclassical value respectively.

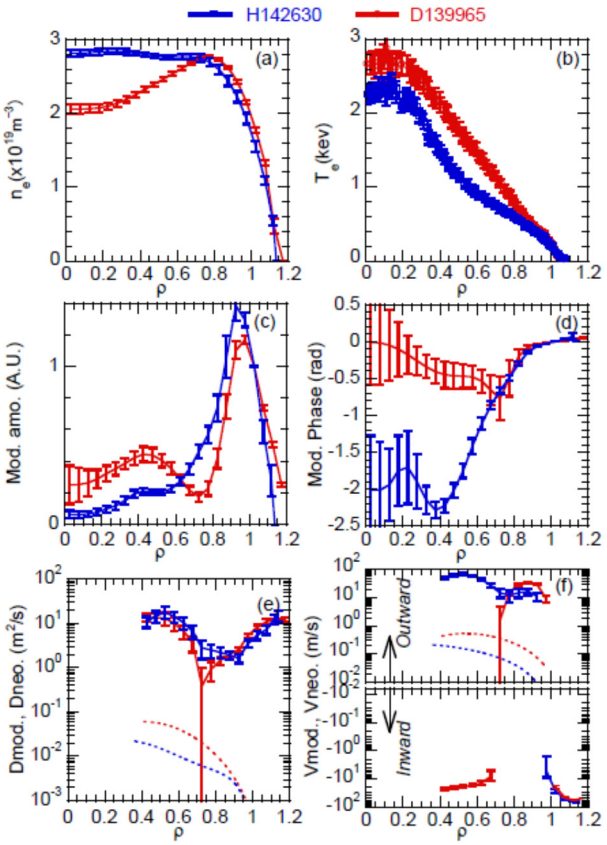

FIG.12 Example of density modulation experiments in high density cases, (a) background ne profiles, (b) background Te profiles (c) modulation amplitude, (d) modulation phase (e) D_{mod}, and (f) V_{mod}. In (e) and (f), plain and dashed lines indicate experimental and neoclassical value respectively

Figure 13 shows the ν_h^* dependence of particle transport coefficients D_{mod} and V_{mod} at $\rho = 0.6$. As shown in Fig.13 (a), the anomalous contribution to diffusion, $D_{mod} - D_{neo}$, increases with of ν_h^* both in H and D plasma. At $\nu_h^* < 3$, D_{mod} in D plasma is higher than in H plasma. At $\nu_h^* > 3$, D_{mod} in D plasma is lower than in H plasma. On the other hand, the ν_h^* and isotope dependence of V_{mod} is more complicated. In the low ν_h^* region, V_{mod} is comparable with V_{neo} in H and D plasma, whilst in high ν_h^* region, V_{mod} much higher and outwards directed in H plasma.

Figure 14 shows ν_h^* dependence of particle transport coefficients at $\rho = 0.9$. As shown in Fig. 13 (a), D_{mod} in H plasma has minimum at $\nu_h^* \sim 1$. At $\nu_h^* > 1$, the anomalous contribution of diffusion increases with increase of ν_h^* both in H and D plasma. At $\nu_h^* = 1 \sim 3$, D_{mod} are comparable in H and D plasma. At $\nu_h^* > 3$, D_{mod} is larger in D plasma than in H plasma. This is opposite tendency compared with ν_h^* dependence at $\nu_h^* > 3$ at $\rho = 0.6$. This suggests that isotope effects of D_{mod} are different at $\rho = 0.6$ and $\rho = 0.9$. Also, determination of a trend in V_{mod} at $\rho = 0.9$ is ambiguous, like at $\rho = 0.6$. As was the case at $\rho = 0.6$, in low ν_h^* region, V_{mod} is comparable with V_{neo} in both H and D plasma. In high ν_h^* region, V_{mod} much more outwardly higher. The cause of the difference of V_{mod} between in H and D plasma are not clear from present dataset.

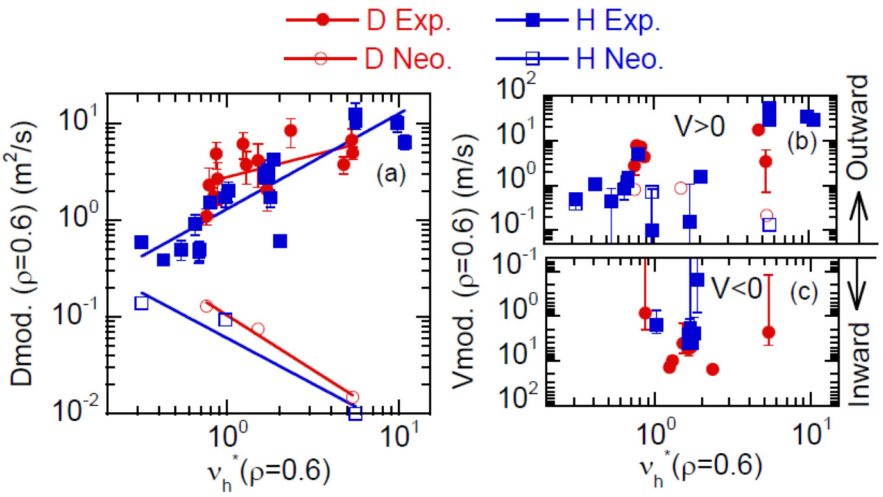

FIG. 13 Collisionality dependence of (a) D_{mod} (ρ=0.6), (b) positive V (ρ=0.6) and (c) negative V (ρ=0.6)

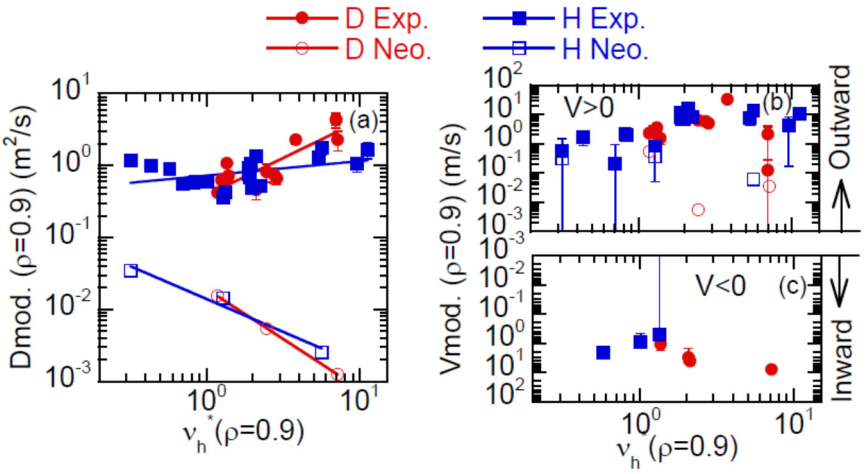

FIG. 14 Collisionality dependence of (a) D(ρ=0.9), (b) positive V(ρ=0.9) and (c) negative V(ρ=0.9)

4. Summary

Extensive investigation of isotope effects in ECRH plasma were performed. Power balance analyses and turbulence analyses are carried out for the data set of density scan with identical ECRH 154GHz ~2MW ρ = 0.1 heating. Ion scale turbulence (k=0.1-0.8m^{-1}) measured by 2D-PCI was higher in D plasma than in H plasma for the low density regime and clearly lower in D plasma than in H plasma for the high density region. The reduction of the ion scale turbulence is evident in core region, where ρ < 0.8. On the other hand, high k turbulence (k=3mm^{-1} and electron scale) measured by high k BS was comparable in low density regime and higher in D plasma in high density regime. Power

balance analysis showed that anomalous contributions of χ_e at $\rho = 0.5\sim0.8$ were comparable between of H and D plasma in low density regime. However, they were clearly reduced in H plasma compared with D plasma in high density regime. Thus, low k ion scale turbulence measured by PCI is likely to play a role on electron transport. The values of χ_i were lower in D plasma than in H plasma over the whole experimental region of ν_h^*. This is due to the lower P_{ei} in D plasma than in H plasma.

Gyrokinetic linear analyses were performed for two cases (low and high density cases) of low k (ITG) and high k (ETG) region in H and D plasma at $\rho = 0.5$ and 0.7. The dominant instability of low k region was ITG. In all cases, growth rate in low k region was lower in D plasma than in H plasma. ITG has gyro-Bohm characteristics, thus, lower growth rate is not due to the difference of the ion species, however is due to the difference of the profiles. In particular, hollower density profile in high density case stabilize ITG and consistent with the reduced ion scale turbulence.

In high k region, ETG was unstable at $\rho = 0.5$ of low density case both in D and H plasma and at $\rho = 0.7$ of high density case both in H and D plasma. At $\rho = 0.7$ of low density case, ETG was stable, however, high k turbulence was clearly measured.

Further gyrokinetic simulation is necessary. The experimental electron and ion heat flux should be validated with gyrokinetic non linear simulation. The particle transports should be investigated from gyrokinetic analyses. In the positive gradient region hollowed density profiles, the dominant instabilities are mainly ITG. ITG driven quasi linear particle flux at positive density gradient region is inwardly directed [48]. Such inwardly directed turbulence driven particle flux can be balanced with outwardly directed neoclassical particle flux in source free region [42,48]. The non linear gyrokinetic simulation will be tried in H and D plasma to understand the particle balance in the source free region. Density modulation experiments were performed for the investigation of isotope effects on particle transport. D_{mod} was anomaly large and anomalous contribution increase with increase of ν_h^* both in H and D plasma. Isotope effects of D_{mod} depend on the location and ν_h^*. At $\rho = 0.6$, D_{mod} is higher at low ν_h^*, and lower at high ν_h^*in D plasma than in H plasma. At $\rho = 0.9$, D_{mod} is comparable in D and H plasma at low ν_h^*, and higher in D plasma than in H plasma at high ν_h^*. T At low ν_h^*, V_{mod} was comparable with V_{neo}, and at high ν_h^*, V_{mod} was clearly higher than V_{neo}. This is common to both $\rho =0.6$ and 0.9.

Isotope effects on transport are evident at high ν_h^* in core region ($\rho < 0.8$). Anomalous χ_e and χ_i reduced and D_{mod} reduced in D plasma compared with H plasma. Key physics quantity is likely to be more hollowed density profile in D plasma. The most important question is why density profile is more hollowed in D plasma. There are no direct isotope effects on linear ITG growth rate. Er does not show clear difference and Er shear is lower than measurements uncertainty. Er shear does not play role. Higher poloidal Mach number ($M_p = V_{ExB}/(\varepsilon_t/q\ V_{ti}) \propto {}^{E}/_{B}\sqrt{m_i/T_i}$, where V_{ExB} is the ExB rotation velocity, εt the toroidal ripple, q the safety factor, the mi ion mass, and the Vti ion

thermal velocity) number has been shown to generate larger zonal flow [49]. This is favorable for heavier ions, however, given V_{EXB}=+-2km/s at ρ=0.7 as shown in Fig. 5 (a-3 and (b-3), M_p is 0.06 in H plasma and 0.08 in D plasma. Such M_p dose not help generation of zonal flow[49]. Also, neoclassical transport does not have isotope effects in i-root at high ν_h^*.

At high ν_h^*, P_{ei} becomes lower in D plasma than in H plasma. Thus, electron heating power (P_e) becomes higher in D plasma. Because of the higher P_e, T_e can be higher. Higher T_e increases V_{neo} in the outwards direction. Conversely, in H plasma, with lower T_e, V_{neo} can be less outwards directed, making density profile less hollow. . This hollower density profile reduces the turbulence. The reduced turbulence reduces anomalous diffusion, then, density profile becomes even more hollow. Such feedback might be possible as shown in Fig.15

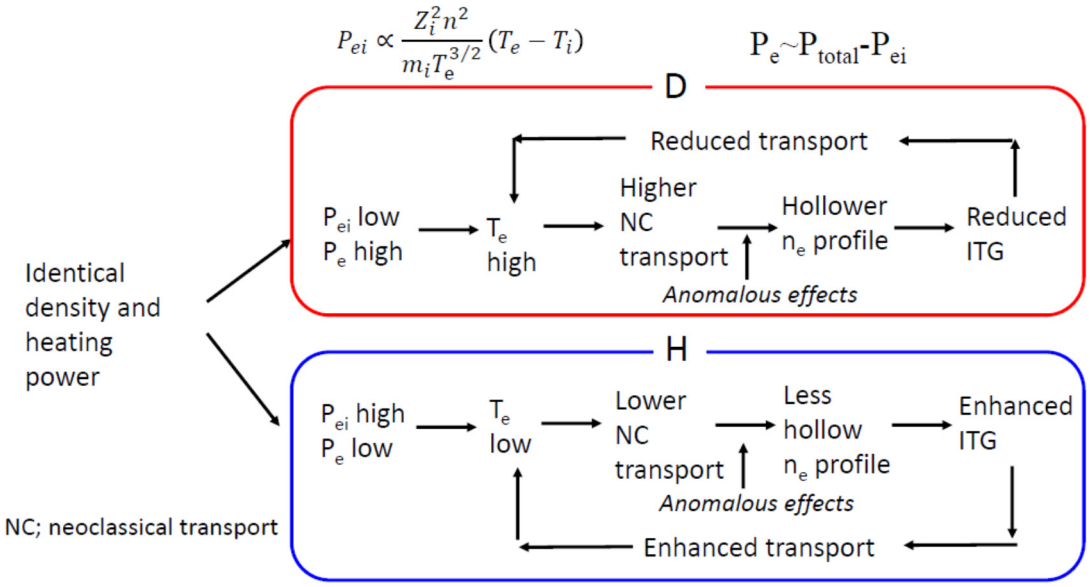

Fig.15 Possible mechanism of isotope effects in high density core region

However, as shown in Fig. 12(b) and 13(b), V_{mod} is much than V_{neo} at high ν_h^* region, where isotope effects are clear , thus, V_{mod} is anomalous. Therefore, a turbulence driven mechanism is necessary to make density profiles hollower in D plasma than in H plasma. Also, conversion from modulation coefficients (D_{mod}, V_{mod}) to equilibrium coefficients (D_{eq}, V_{eq}) will help the understanding of difference of density profile. Such conversions are possible by the grad n_e integration for D_{mod} and n_e integration for V_{mod} [48]. These further investigation is necessary for the next step.

Generation of the zonal flow could play a role in the isotope effects. Presently, turbulence drive zonal flow was not yet measured. Measurements using heavy ion beam probe should be tried. Alternatively, fluctuation of phase velocity from PCI could show zonal flow. This requires high time

resolution of phase velocity measurements and need further development of diagnostics and analyses technique.

ACKNOWLEDGMENTS

This work is supported by NIFS grants NIFS17ULHH013, NIFS18ULHH013, NIFS18KLER045, NIFS18KLPH032, NIFS18KUHL083, NIFS19KLPH038 and JSPS grant 16H04620. This work is supported by the US DOE under DE-SC0019007

References

[1] Maggi C F et al, Plasma Phys. Control. Fusion 60 (2018) 014045

[2] Urano H et al 2012 Phys. Rev. Lett. 109 125001

[3] Urano H et al 2013 Nucl. Fusion 53 083003

[4] Schneider P et al 2017 Nucl. Fusion 57 066003

[5] Maggi C F et al 2019 Nucl. Fusion 59 076028

[6] Takahashi H et al, Nucl. Fusion **58** (2018) 106028

[7] Kobayashi T et al, Plasma Phys. Control. Fusion 61 (2019) 085005

[8] Nagaoka K et al, to be published Nucl. Fusion

[9] Yamada H et al tobe published Phys. Rev. Lett.

[10] Warmer F et al, Nucl. Fusion **58** (2018)106025

[11] Tanaka K et al, to be published Nucl. Fusion https://doi.org/10.1088/1741-4326/ab4237

[12] Igami H et al EPJ Web of Conferences **203**, 02001 (2019) https://doi.org/10.1051/epjconf/201920302001

[13] Yamada H. et al 2005 Nucl. Fusion 45 1684

[14] Tanaka K et al Rev. Sci. Instrum. **79**, (2008), 10E702

[15] Michael C A et al Rev. Sci. Instrum. **86**, (2015), 093503

[16] Tokuzawa T et al Proceedings of 43rd International Conference on Infrared, Millimeter, and Terahertz Waves (IRMMW-THz 2018) Sep. 9 - 14, 2018 at Nagoya Congress Center Nagoya, Japan

[17] Tanaka K, et al, Plasma Fusion Res **3**, (2008) 050

[18] Yamada I et al, Fusion Sci. Tech. **58**, (2010) 345

[19] Yoshinuma M et al, Fusion Sci. Tech. **58**, (2010) 37

[20] Seki R. et al 2011 Plasma Fusion Res. 6 2402081

[21] Beidler C. D. et al, Plasma Phys. Control. Fusion, 36, (1994), 317

[22] Wesson J.A., 1997 Tokamaks 2nd edition (Oxford: Clarendon)

[23] Yokoayama M et al Nucl. Fusion 47 (2007) 1213

[24] Matsuoka S et al, Plasma Fusion Res. 3 (2008) S1056

[25] Dinklage A et al Nucl. Fusion 53 (2013) 063022

[26] Huang B et al Phys. Plasmas 24, 022503 (2017);

[27] Satake S et al, presented at international Toki conference 2017

[28] Mikkelsen D.R. et al, Physics of Plasmas 21, 082302 (2014)

[29] Takahashi H et al, Nucl. Fusion 57 (2017) 086029

[30] Michael C A Plasma Fusion Res. 2, S1034 (2007)

[31] Nunami M et al, Plasma Fusion Res. 5, 016 (2010)

[32] Nakata M et al, Plasma Phys. Ctrl. Fusion 61 (2019) 014016

[33] Nakata M et al, Phys. Rev. Lett. 118, (2017), 165002

[34] Plunk G.G. et al, Phys. Rev. Lett. 122, (2019) 035002

[35] Shats M G et al, Phys. Plasmas 2, (1995), 398

[36] Deng C. B. et al 2015 Nucl. Fusion 55 (2015)123003

[37] Estrada T et al Nucl. Fusion 59 (2019) 076021

[38] Murakami S et al Nucl. Fusion **42**, (2002) L19–L2

[39] Yokoyama M et al, J. Plasma Fusion Res. **81**, (2005) 83

[40] Gentle K.W. et al, Plasma Phys. Control. Fusion **29** (1987) 1077

[41] Lopes, N. J. C. Plasma Phys. Control. Fusion **37** (1995) 799

[42] Tanaka K. et al, Fusion Sci. Tech. **58**, (2010), 70

[43] Gentle K.W. et al, Nucl. Fusion **22** (1992) 217

[44] Tanaka K et al, Plasma Phys. Control. Fusion **58** (2016) 055011

[45] Ohtani Y et al, J. Phys. Soc. Jpn. **86** (2017) 06451

[46] Ohtani Y et al, submitted Plasma Phys. Ctrl. Fusion

[47] Shoji M et al. J. Nucl. Mater., 363-365:827 – 832, (2007)

[48] Yamagishi O et al Phys. Plasmas 14 (2007) 012505

[49] Watanabe T H et al, Nucl. Fusion 51 (2011) 123003

[50] Tala Tet al, to be published Nucl. Fusion https://doi.org/10.1088/1741-4326/ab4248"